Electronic Supplementary Material (ESI) for Biomaterials Science.

Supporting Information

Single-tailed Heterocyclic Carboxamide Lipids for Macrophage Immune-Modulation

Kuo-Ching Mei,[a,b]* Rebeca T. Stiepel,[a] Emily Bonacquisti,[a] Natalie E. Jasiewicz,[a] Ameya Pravin Chaudhari,[2] Palas B. Tiwade,[a] Eric M. Bachelder,[a] Kristy M. Ainslie,[a] Owen S. Fenton,[a] Juliane Nguyen[a]*

a Division of Pharmacoengineering and Molecular Pharmaceutics, Eshelman School of Pharmacy, University of North Carolina at Chapel Hill, Chapel Hill, NC, USA

b Department of Pharmaceutical Sciences, School of Pharmacy and Pharmaceutical Sciences, State University of New York at Binghamton, Binghamton, NY, USA

* Correspondence to julianen@email.unc.edu and kmei@binghamton.edu

List of Supporting Figures and Tables

Methods for Lipid Synthesis and Purification

Heterocyclic carboxamide lipids were synthesized in two steps: (i) 1,2-epoxytetradecane (1 e.q., transparent oil) was mixed with propargylamine (1 e.q., yellow-ish oil) in microreactor vials without additional solvents and heated at 80 ^{o}C for 72 h under constant stirring to facilitate the nucleophilic epoxy ring-opening via an amine. The reaction was cooled to room temperature to produce the waxy crudes, which were further purified using normal phase flash chromatography (EtOAc: Hexane, gradient mode) to produce the ionizable propargyl lipid **KM1** as a white powder (yield >85%, Rf = 0.25 when EtOAc: hexane = 1:1 v/v). (ii) Heterocyclic carboxamide lipids were synthesized via a nucleophilic addition/elimination reaction between acid chlorides and amines. In brief, lipid **KM1** (1 e.q.) was dissolved in dichloromethane, followed by the addition of heterocyclic carbonyl chloride building blocks (1.2 e.q.), *i.e.,* 1-pyrrolidinecarbonyl chloride, 4-morpholinecarbonyl chloride, and 4-methyl-1-piperazinecarbonyl chloride. Solvents were evaporated after stirring the reaction solution for 24 h at room temperature. The reaction crudes were purified by normal phase flash chromatography (EtOAc: hexane, gradient mode) to produce heterocyclic carboxamide lipids **KM2** (yield = 83%, Rf = 0.41, EtOAc: hexane = 1:1 v/v) and **KM3** (yield = 74%, Rf = 0.41, EtOAc: hexane = 1:1 v/v). Lipid **KM4** was purified using MeOH: CH_2Cl_2: conc. NH_4OH = 22: 75:3 v/v, 0-60% v/v against CH_2Cl_2 (yield = 33%, Rf = 0.65, MeOH: CH_2Cl_2: conc. NH_4OH = 11:87.5: 1.5 v/v). The ^{1}H NMR, ^{1}H-^{1}H COSY-NMR, ^{13}C NMR, and ESI-MS spectra of the lipids can be found in the online Supporting Information (Figures **S1 – S16**). All lipids were screened for endotoxin after purification using the Pierce™ Chromogenic Endotoxin Quant kit (ThermoFisher Scientific). All samples had undetectable levels of endotoxin (< 0.1 EU/mg).

Endotoxin All lipids were screened for endotoxin levels before biological studies using Pierce™ Chromogenic Endotoxin Quant Kit following the manufacturer's instructions (ThermoFisher # A39552, detection ranges: 0.01 EU/mL to 1 EU/mL). Lipids with < 0.1 EU/mL of endotoxin levels were used for downstream cell-based studies. Lipids with > 0.1 EU/mL of endotoxin levels are re-purified using flash chromatography (Biotage).

Methods for Biological Studies

General Cell Culture DC2.4 (Sigma, # SCC142) cells were cultured in RPMI-1640 (Gibco # 11835030) supplemented with 10% v/v/ fetal bovine serum (Sigma #ES-009-B), 1X Glutagro (Corning # 25-015-CI), 1X non-essential amino acids (Gibco # 11140050), 1X HEPES buffer solution (Sigma, #TMS-003-C), 1% Penicillin-Streptomycin (P/S, Gibco# 15140163), and 0.0054X beta-mercaptoethanol (Sigma #ES-007-E). NF-KB Renilla Luciferase Reporter-RAW264.7 (Crownbio, #C3001) cells were cultured in DMEM (Gibco # A1896701), supplemented with 10% v/v FBS, 1% v/v P/S, and 3 µg/ml of Puromycin (ThermoFisher # J67236.8EQ, puromycin included for cell expansion only, not for viability, RT-PCR, and cytokine release studies). Both cells were maintained in a humidified cell culture incubator at 37^{o}C with 5% CO_2.

Viability Studies RAW and DC2.4 cells were seeded with phenol red-free media in standard 96-well plates (10,000 cells/well) and left overnight before use. Cells were treated with 14:0 LysoPC (control group) and KM lipids for 24 h. Viability studies were performed using MTS assay following the manufacturer's instruction (Promega, CellTiter 96 AQueous MTS Reagent Powder, Promega; Phenazine methosulfate, Sigma #9625).

RT-PCR Studies RAW and DC2.4 cells were seeded with phenol red-free media in standard 24-well plates (0.1 x 10^6 cells/well) and left overnight before use. Culture media were replaced with fresh media the next day before lipid treatments. After 6 h incubation, supernatants were removed. Cells were gently washed with PBS three times before being lysed for RNA isolation using RNeasy mini kit following the manufacturer's instructions (Qiagen, # 74104). cDNA was synthesized from the isolated RNA using the iScript™ cDNA synthesis kit (Bio-Rad # 1708891). Forward and reverse RT-PCR primers (ordered from IDT) were mixed with iTaq Universal SYBR Green Supermix (Bio-Rad # 1725121) and amplified/detected in an RT-PCR system (QuantStudio 3™), then analyzed using Design and Analysis Software v1.5.2.

Cytokine Release Cell culture media from the RT-PCR studies were collected for cytokine-release studies. This study used Luminex xMAP technology for multiplexed quantification of mouse cytokines, and the multiplexing analysis was performed using the Luminex™ 200 system (Luminex, Austin, TX, USA) by Eve Technologies Corp. (Calgary, Alberta).

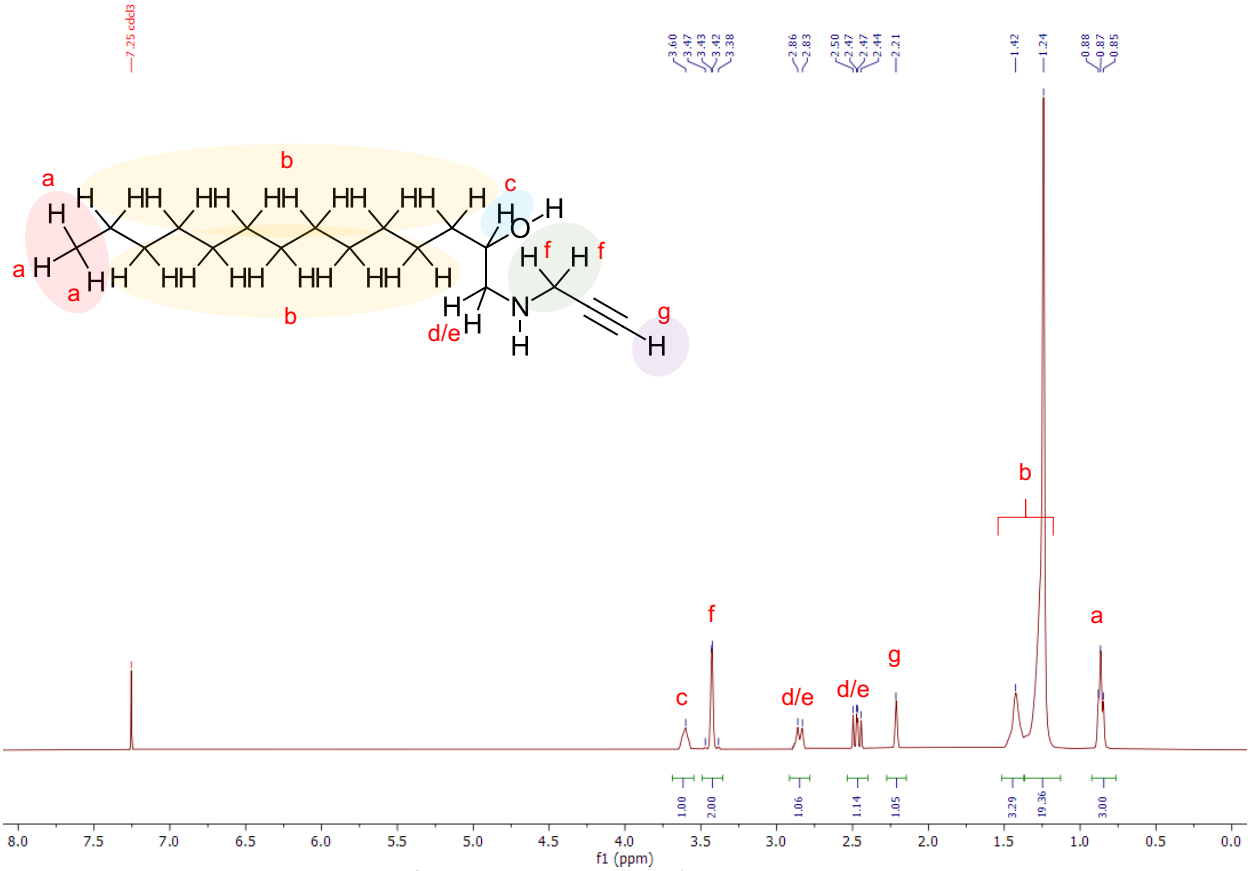

Figure S1. NMR Spectrum (^{1}H) of Lipid KM1. ^{1}H NMR (400 MHz, $CDCl_3$) δ 3.60 (s, 1H), 3.43 (d, *J* = 1.8 Hz, 2H), 2.85 (d, *J* = 12.2 Hz, 1H), 2.47 (dd, *J* = 12.1, 9.2 Hz, 1H), 2.21 (s, 1H), 1.42 (s, 3H), 1.24 (s, 19H), 0.86 (t, *J* = 6.6 Hz, 3H).

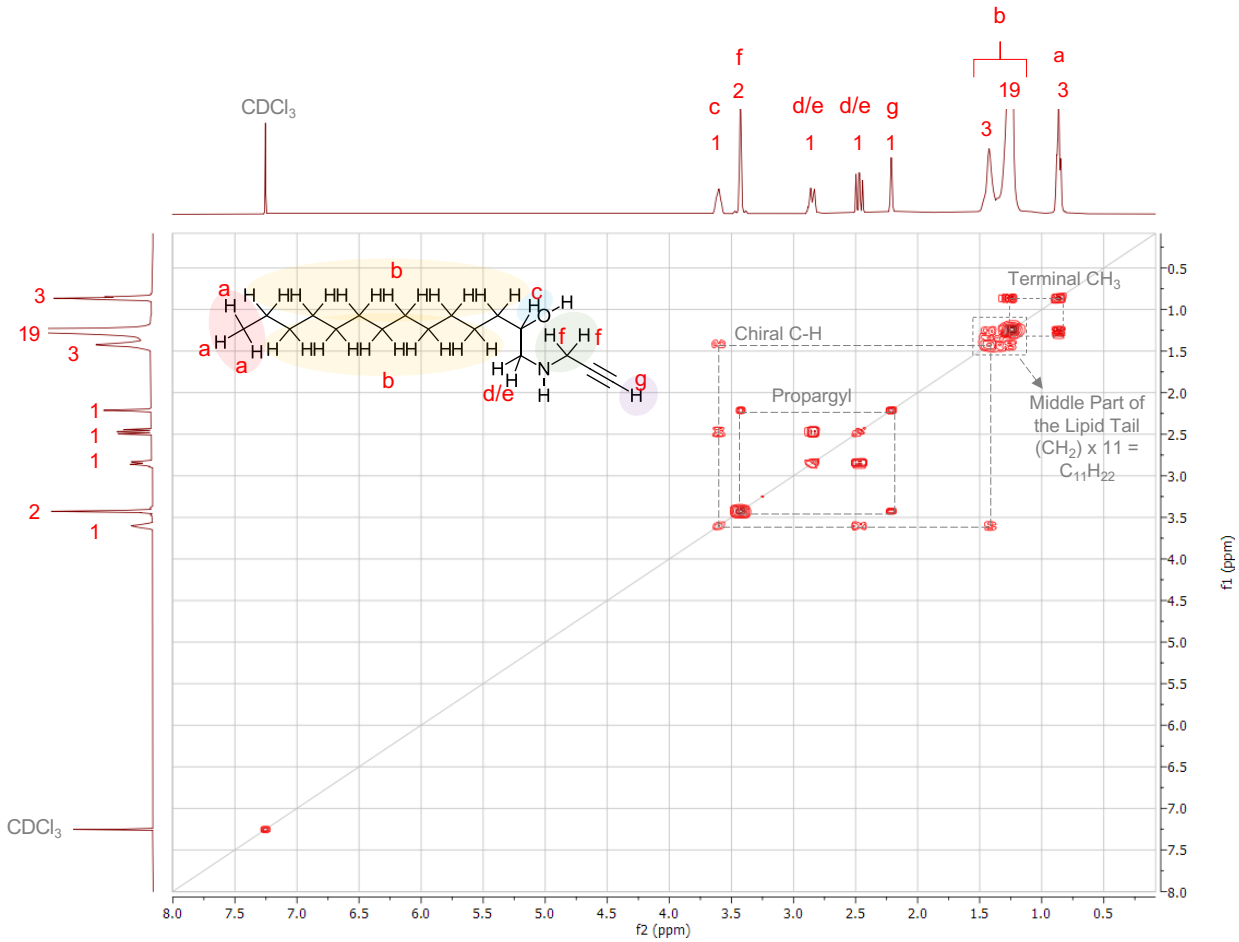

Figure S2. NMR Spectrum (^{1}H-^{1}H Correlated Spectroscopy/COSY) NMR of Lipid KM1.

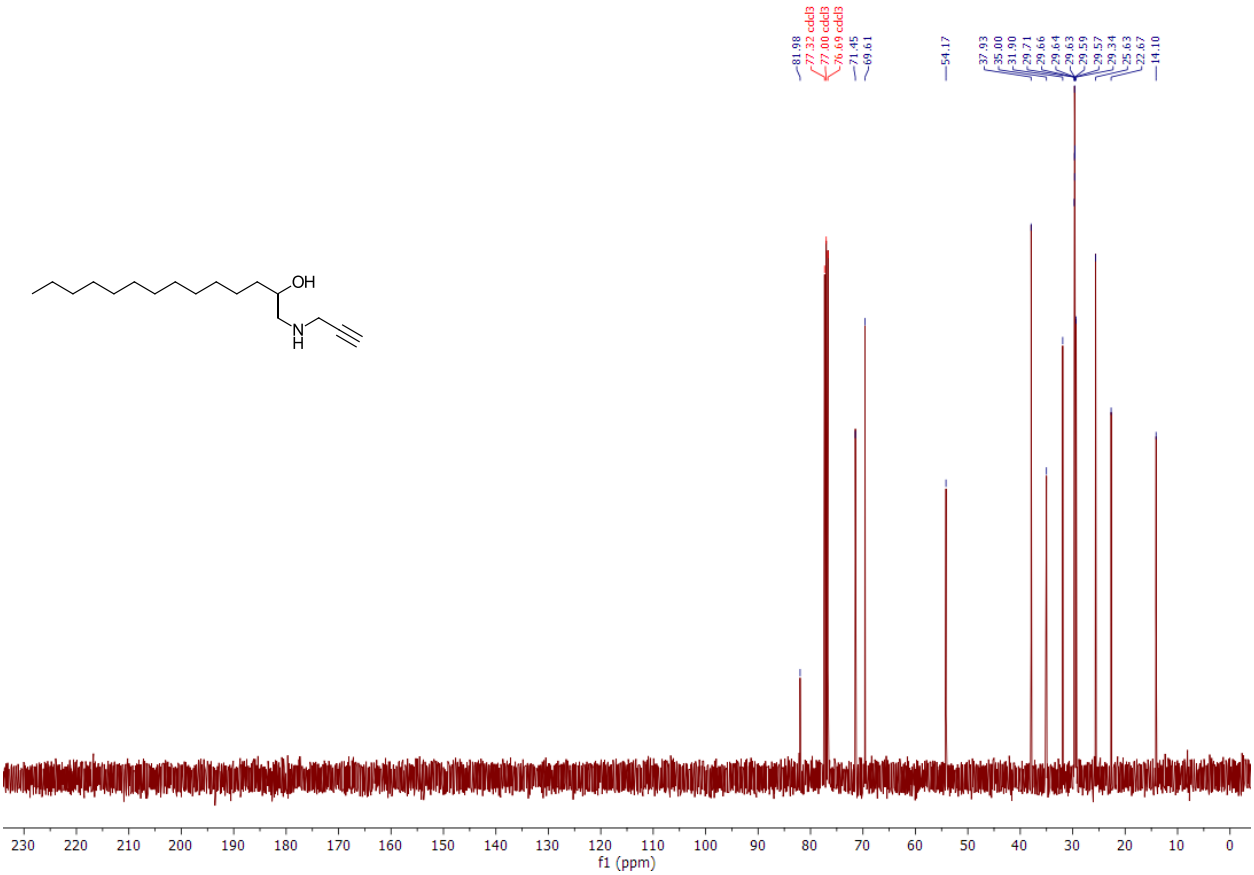

Figure S3. NMR Spectrum (^{13}C) of Lipid KM1. ^{13}C NMR (101 MHz, $CDCl_3$) δ 81.98, 71.45, 69.61, 54.17, 37.93, 35.00, 31.90, 29.71, 29.66, 29.64, 29.63, 29.59, 29.57, 29.34, 25.63, 22.67, 14.10.

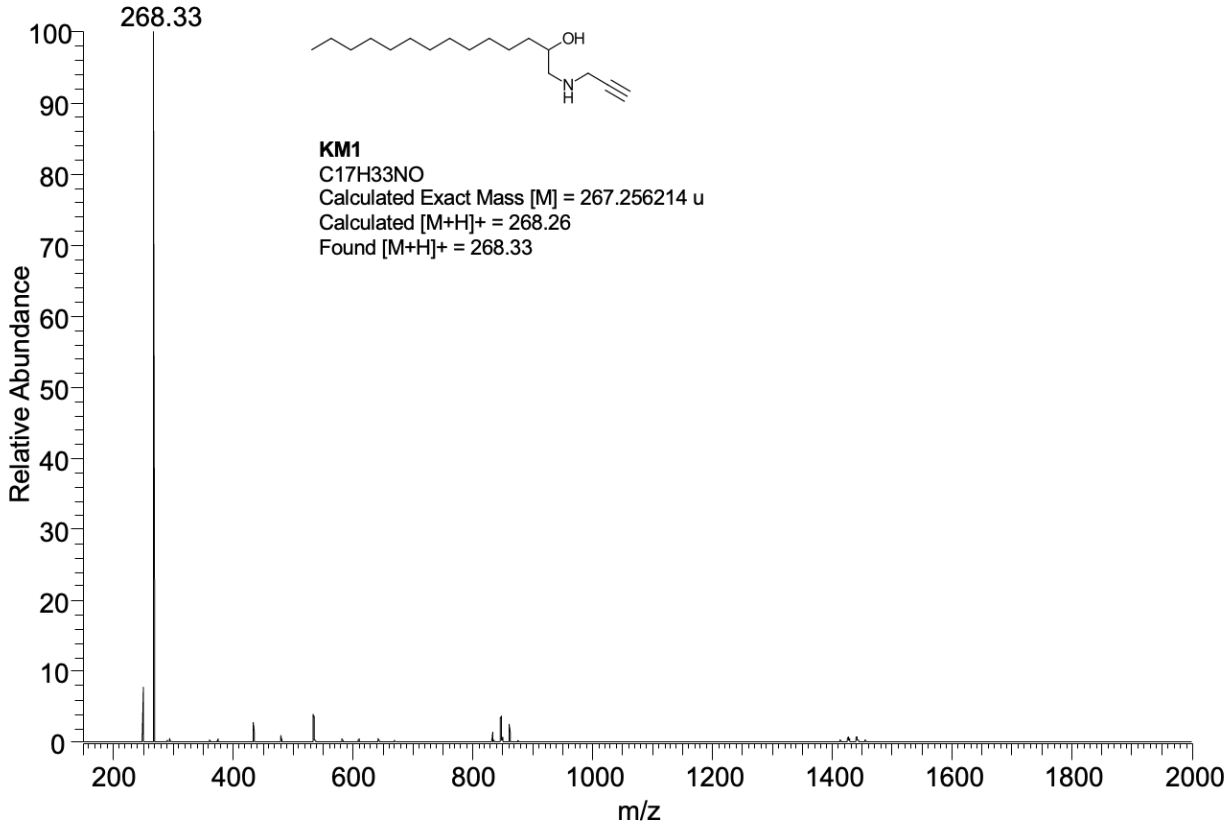

Figure S4. ESI-MS Spectrum of Lipid KM1.

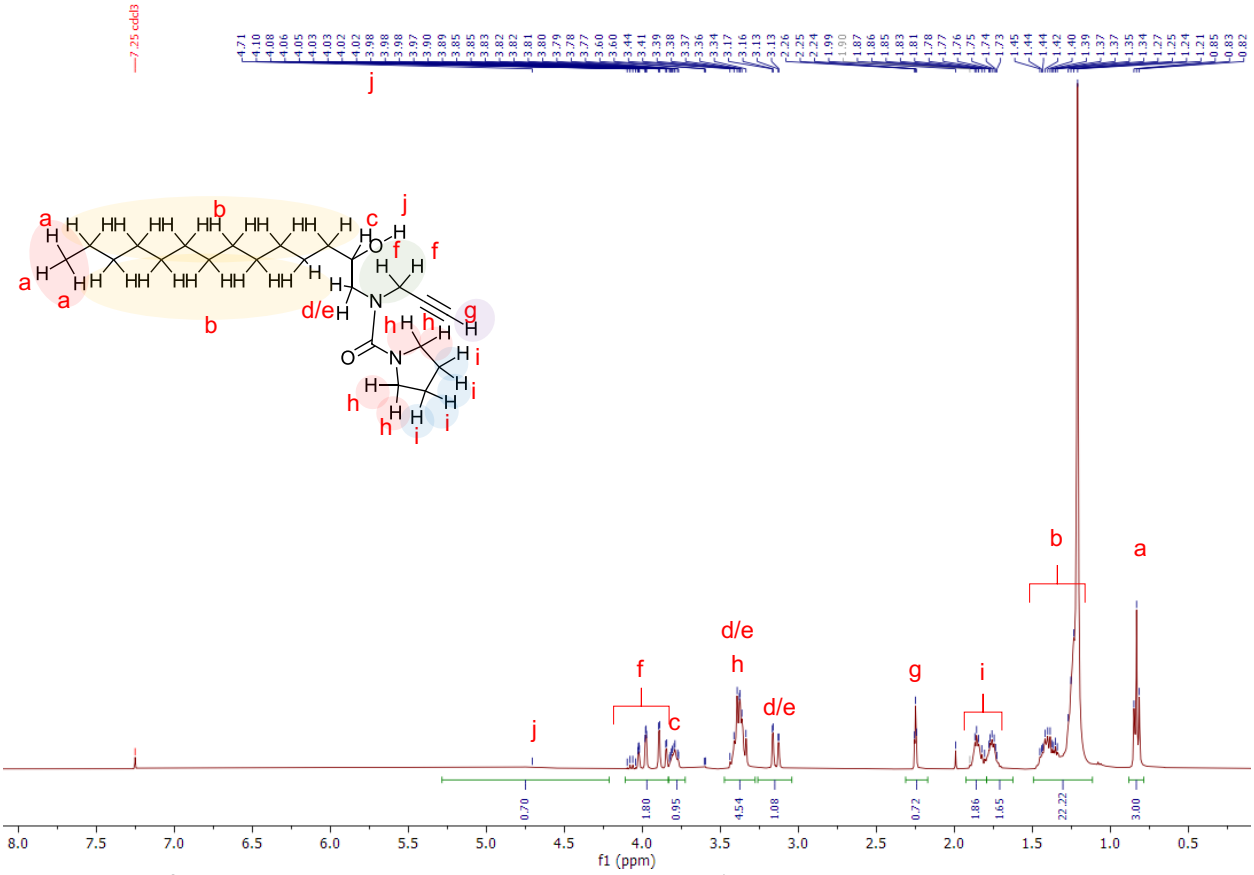

Figure S5. ^{1}H NMR of Lipid KM2 ($C_{22}H_{40}N_2O_2$). ^{1}H NMR (400 MHz, $CDCl_3$) δ 4.71 (s, 1H), 4.11 – 3.83 (m, 2H), 3.83 – 3.73 (m, 1H), 3.48 – 3.28 (m, 5H), 3.15 (dd, *J* = 14.8, 2.2 Hz, 1H), 2.25 (t, *J* = 2.4 Hz, 1H), 1.93 – 1.79 (m, 2H), 1.79 – 1.63 (m, 2H), 1.49 – 1.12 (m, 22H), 0.88 – 0.79 (m, 3H).

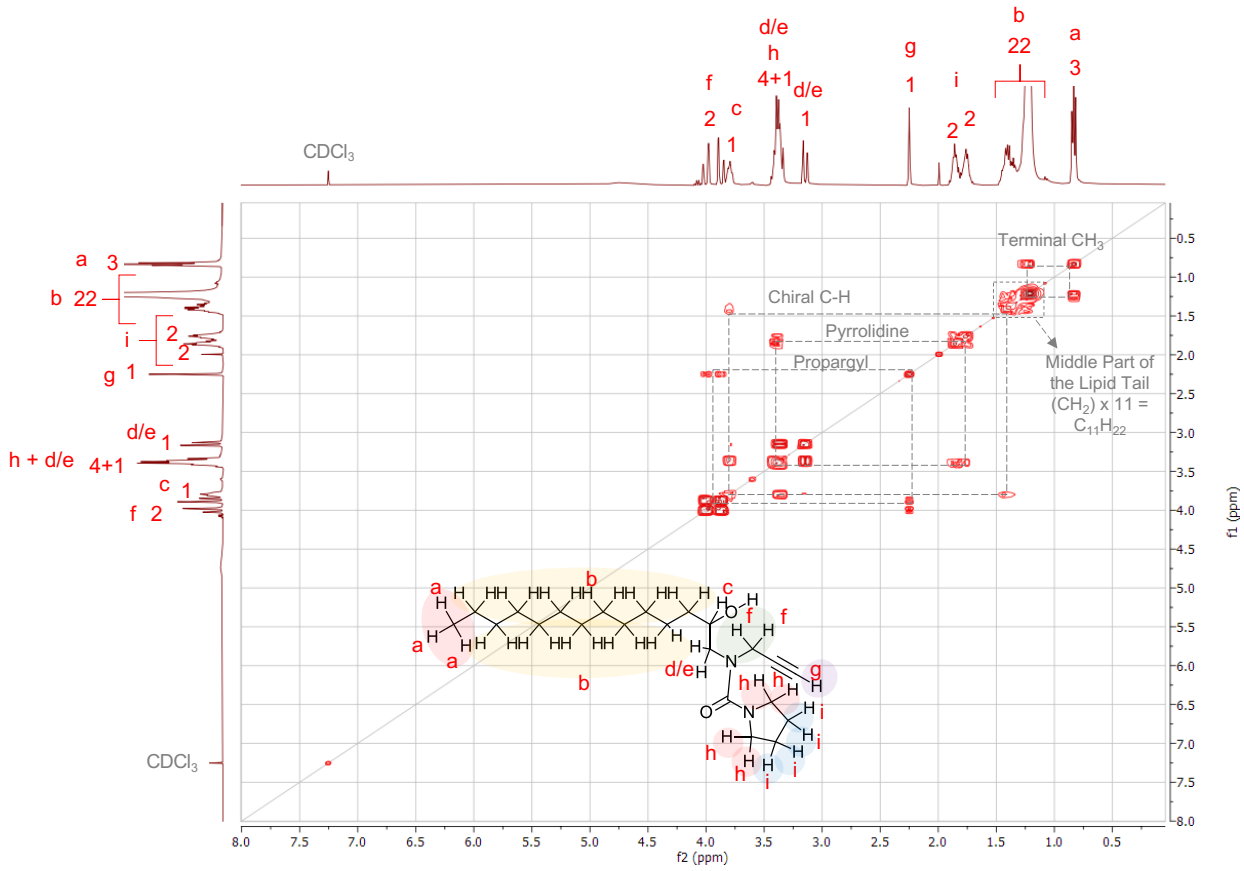

Figure S6. NMR Spectrum (COSY) of Lipid KM2.

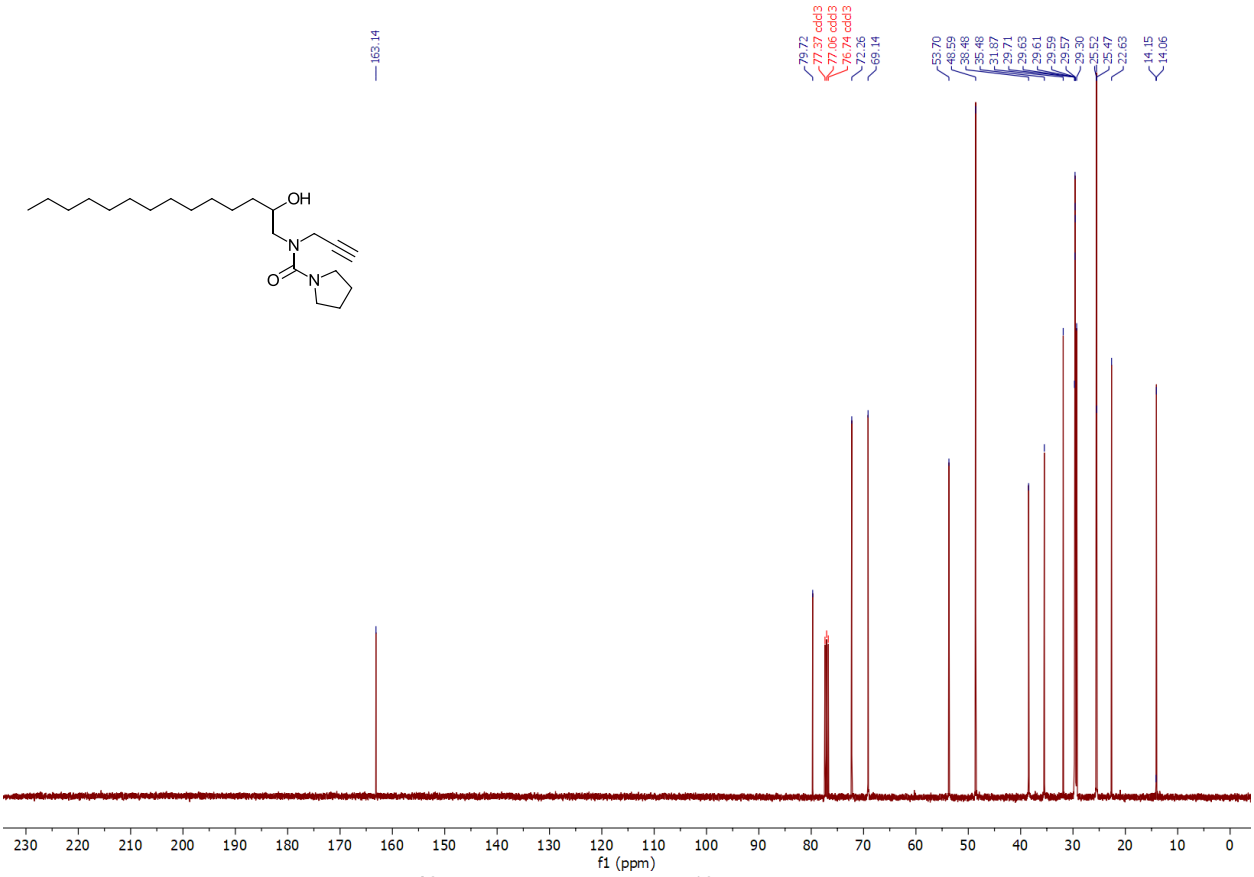

Figure S7. NMR Spectrum (^{13}C) of Lipid KM2. ^{13}C NMR (101 MHz, $CDCl_3$) δ 163.14, 79.72, 72.26, 69.14, 53.70, 48.59, 38.48, 35.48, 31.87, 29.71, 29.63, 29.61, 29.59, 29.57, 29.30, 25.52, 25.47, 22.63, 14.15, 14.06.

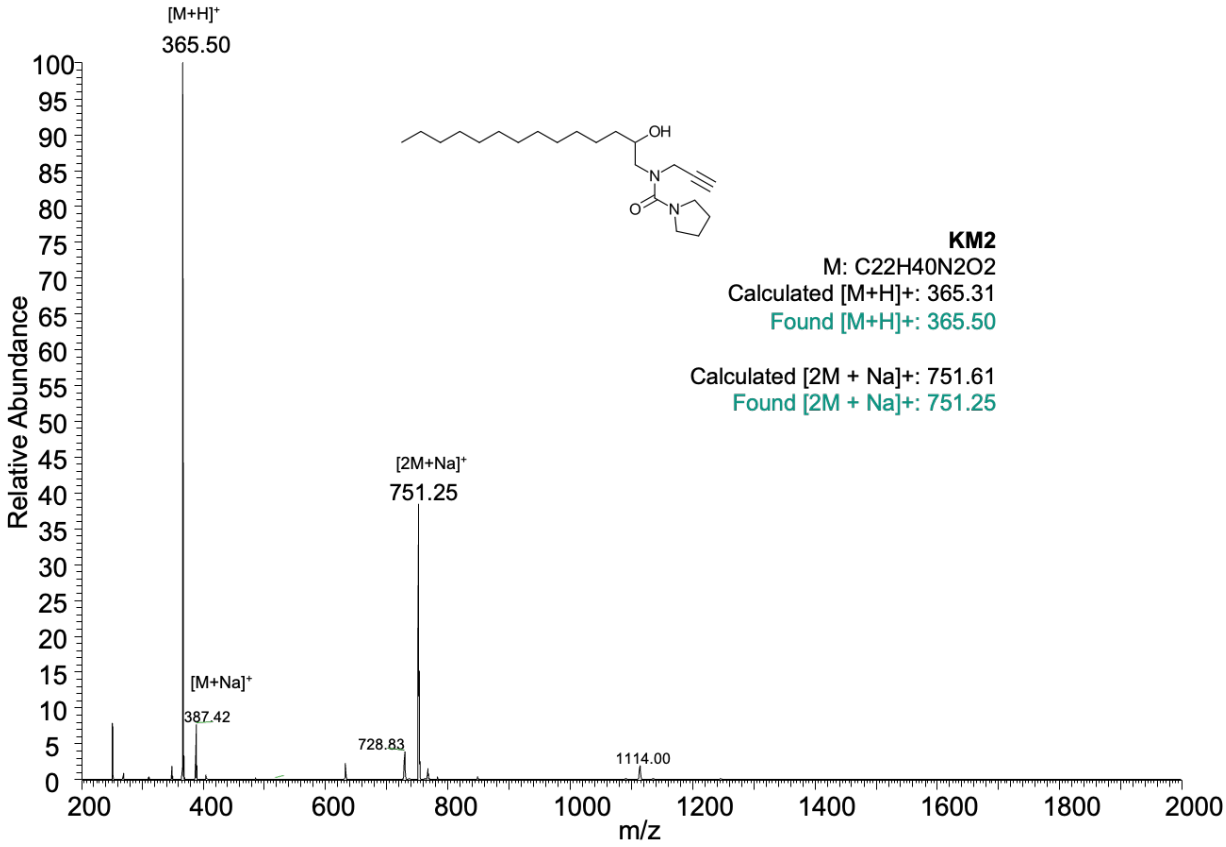

Figure S8. ESI-MS Spectrum of Lipid KM2.

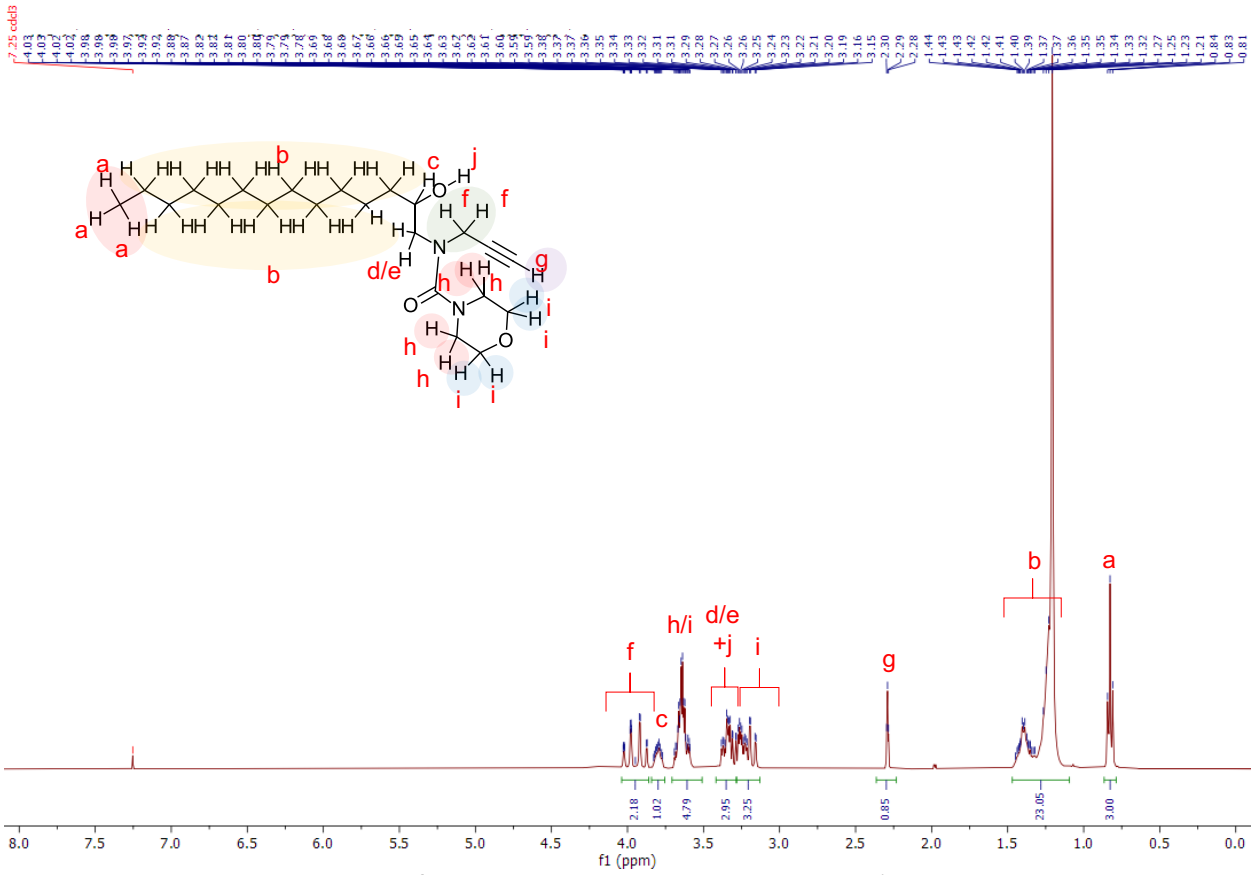

Figure S9. NMR Spectrum (^{1}H) of Lipid KM3 ($C_{22}H_{40}N_2O_3$). ^{1}H NMR (400 MHz, cdcl$_3$) δ 4.04 – 3.86 (m, 2H), 3.84 – 3.76 (m, 1H), 3.71 – 3.51 (m, 5H), 3.35 (ddd, *J* = 13.7, 6.3, 3.6 Hz, 2H), 3.32 – 3.11 (m, 4H), 2.29 (t, *J* = 2.4 Hz, 1H), 1.47 – 1.09 (m, 23H), 0.83 (t, *J* = 6.8 Hz, 3H).

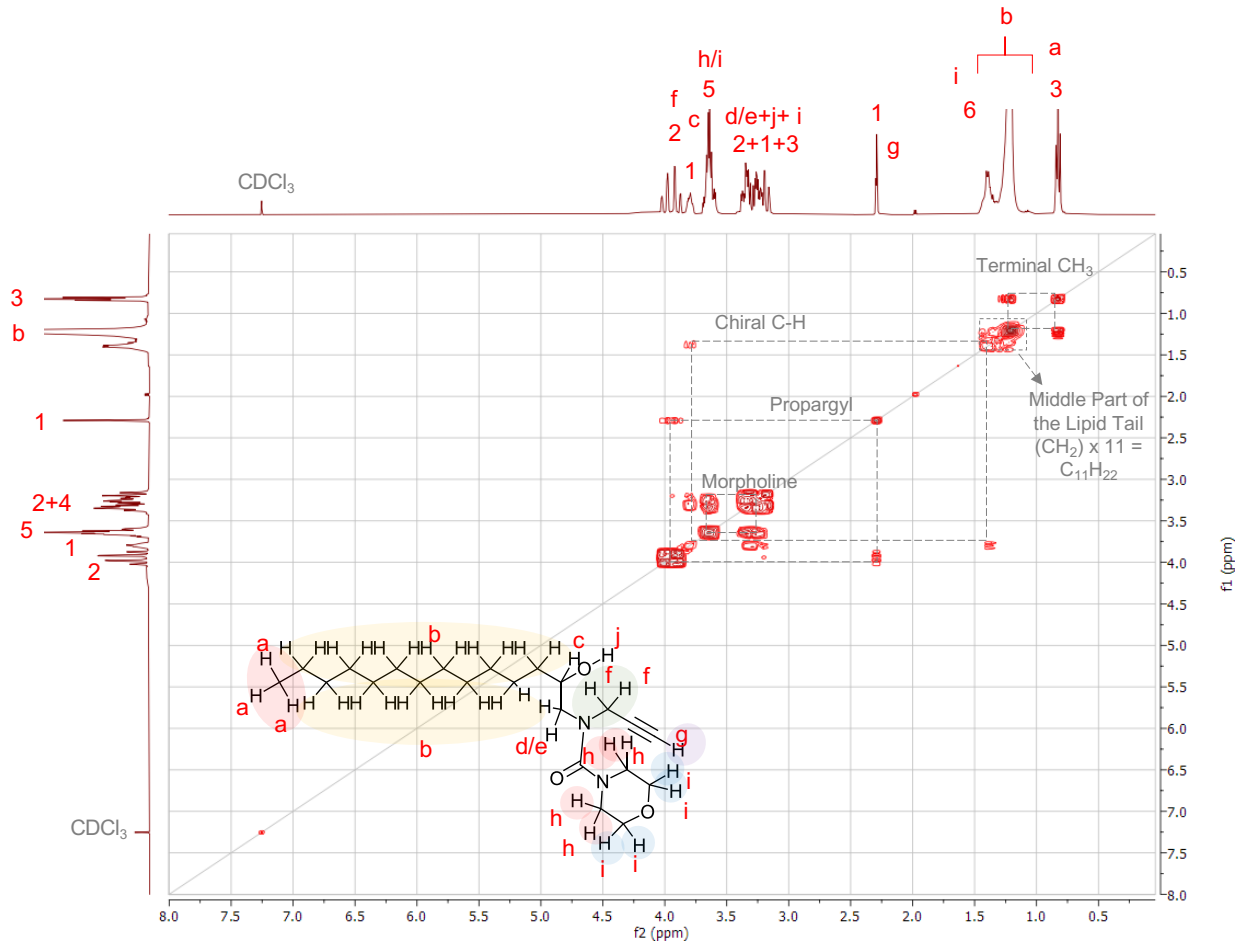

Figure S10. NMR Spectrum (COSY) of Lipid KM3.

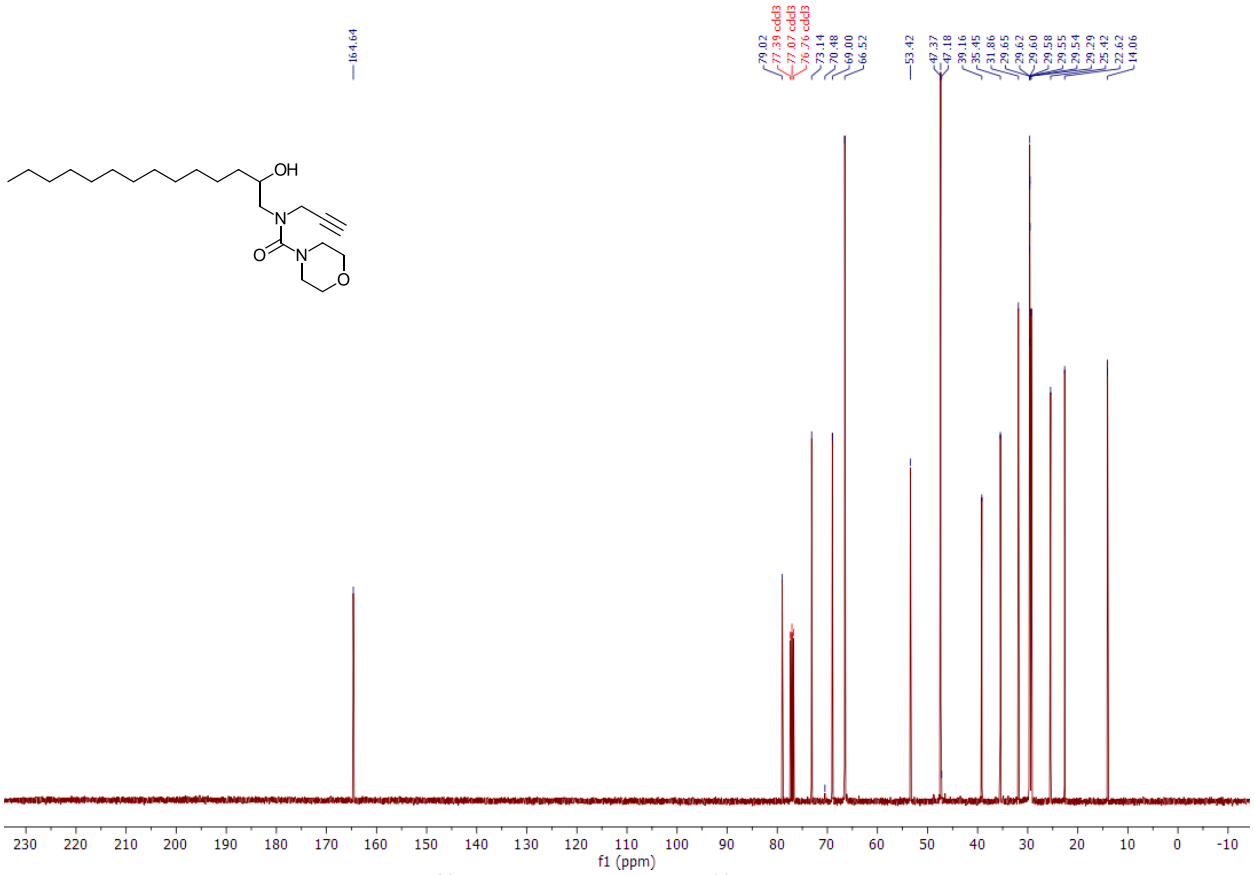

Figure S11. NMR Spectrum (^{13}C) of Lipid KM3. ^{13}C NMR (101 MHz, $cdcl_3$) δ 164.64, 79.02, 73.14, 70.48, 69.00, 66.52, 53.42, 47.37, 47.18, 39.16, 35.45, 31.86, 29.65, 29.62, 29.60, 29.58, 29.55, 29.54, 29.29, 25.42, 22.62, 14.06.

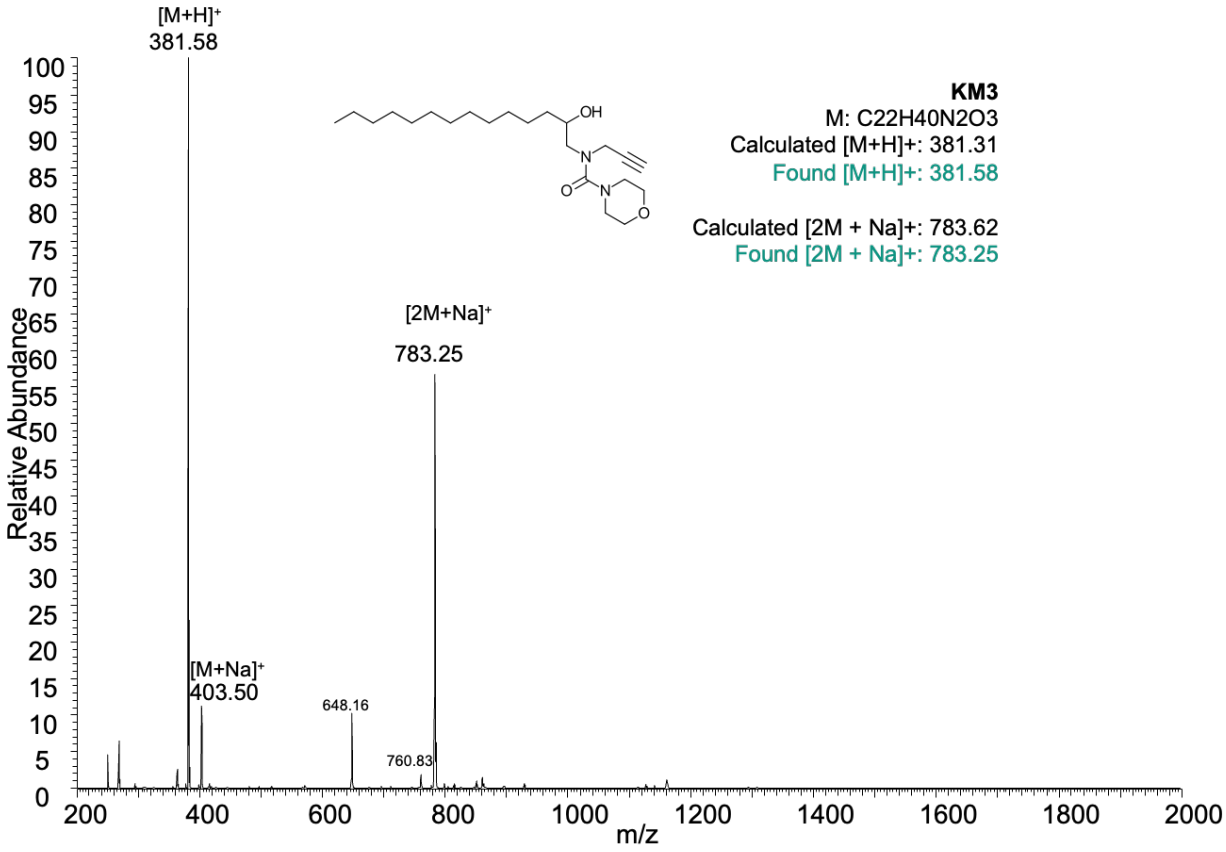

Figure S12. ESI-MS Spectrum of Lipid KM3.

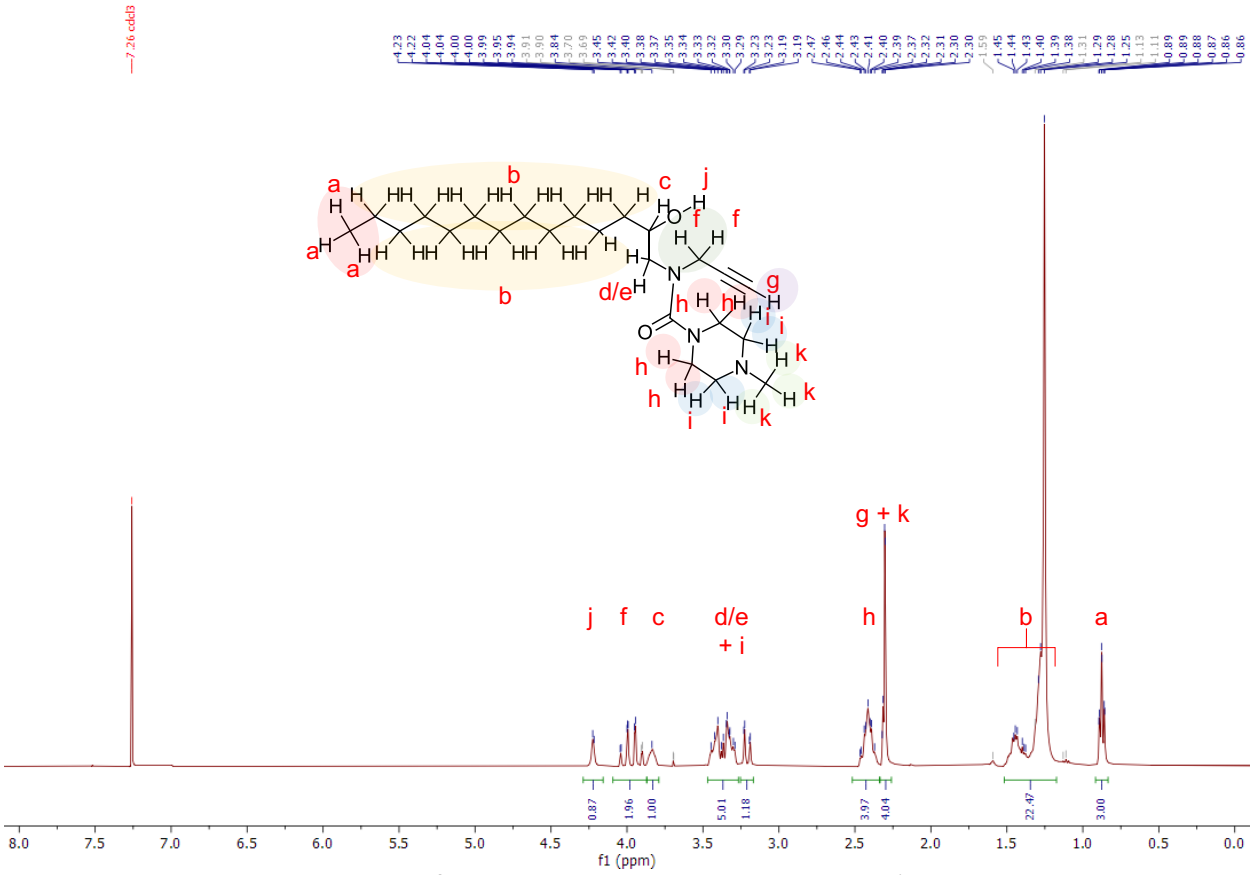

Figure S13. NMR Spectrum (^{1}H) of Lipid KM4 ($C_{23}H_{43}N_3O_2$). ^{1}H NMR (400 MHz, $cdcl_3$) δ 4.22 (d, *J* = 3.4 Hz, 1H), 4.09 – 3.87 (m, 2H), 3.84 (s, 1H), 3.47 – 3.27 (m, 5H), 3.21 (dd, *J* = 14.7, 2.3 Hz, 1H), 2.42 (ddt, *J* = 17.5, 11.7, 5.7 Hz, 4H), 2.33 – 2.26 (m, 4H), 1.52 – 1.17 (m, 22H), 0.88 (td, *J* = 6.9, 1.3 Hz, 3H).

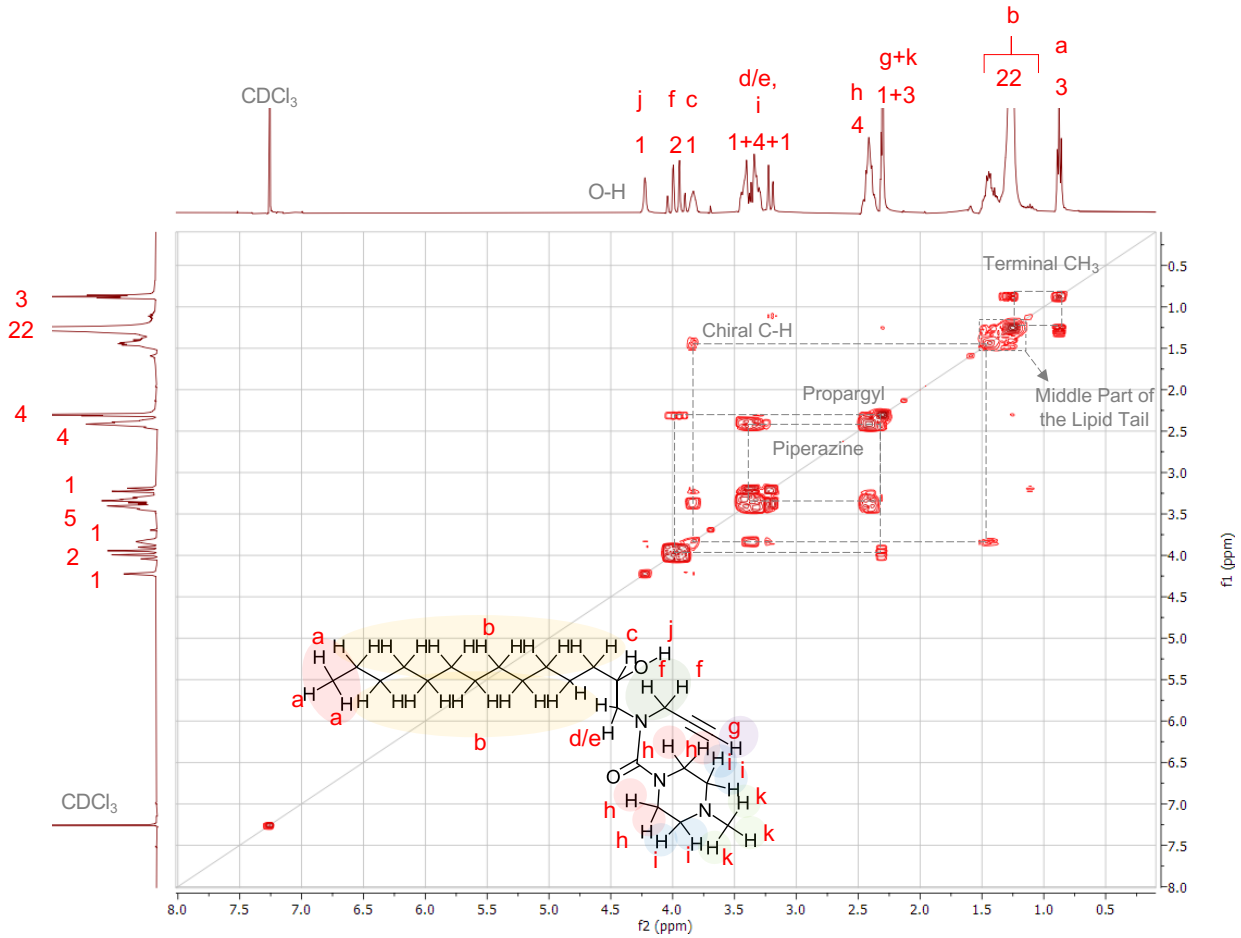

Figure S14. NMR Spectrum of Lipid KM4.

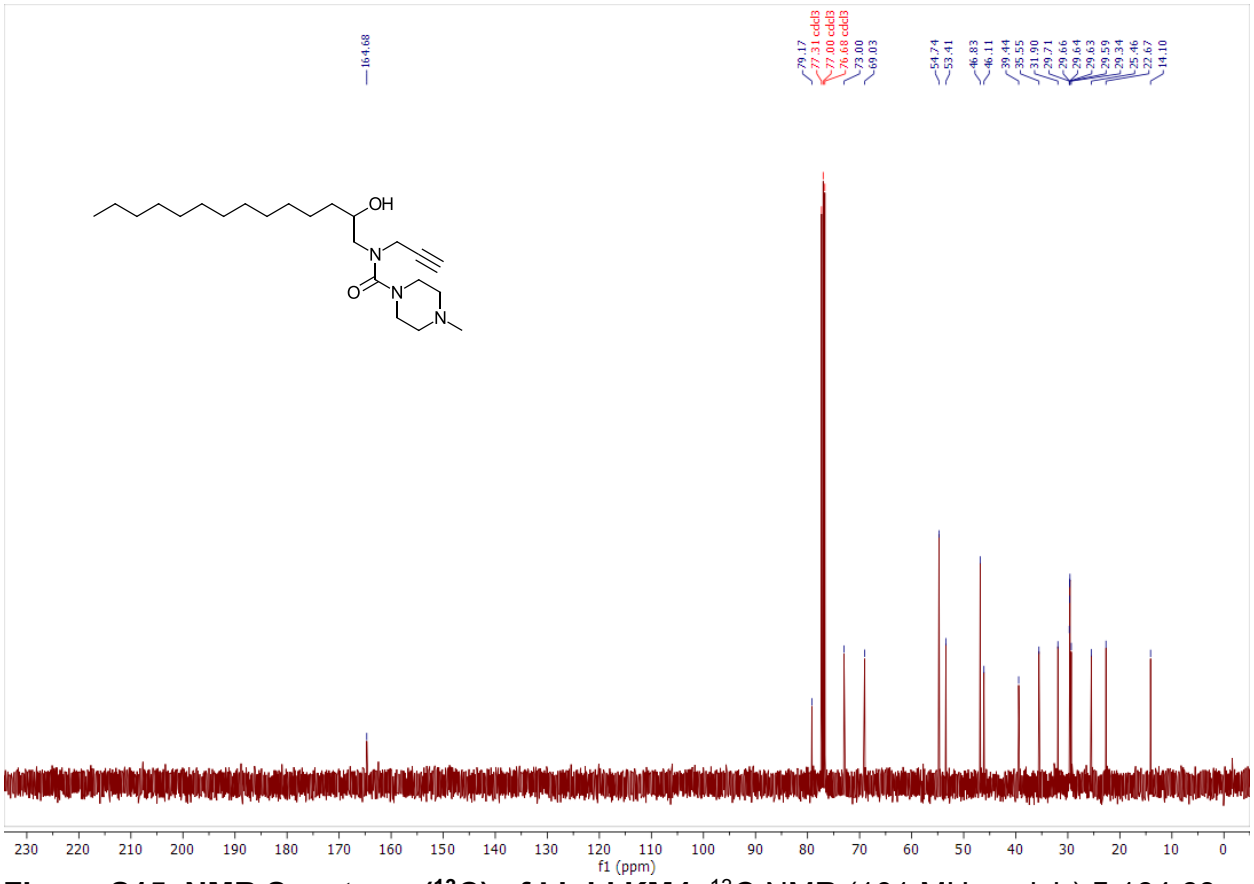

Figure S15. NMR Spectrum (^{13}C) of Lipid KM4. ^{13}C NMR (101 MHz, $cdcl_3$) δ 164.68, 79.17, 73.00, 69.03, 54.74, 53.41, 46.83, 46.11, 39.44, 35.55, 31.90, 29.71, 29.66, 29.64, 29.63, 29.59, 29.34, 25.46, 22.67, 14.10.

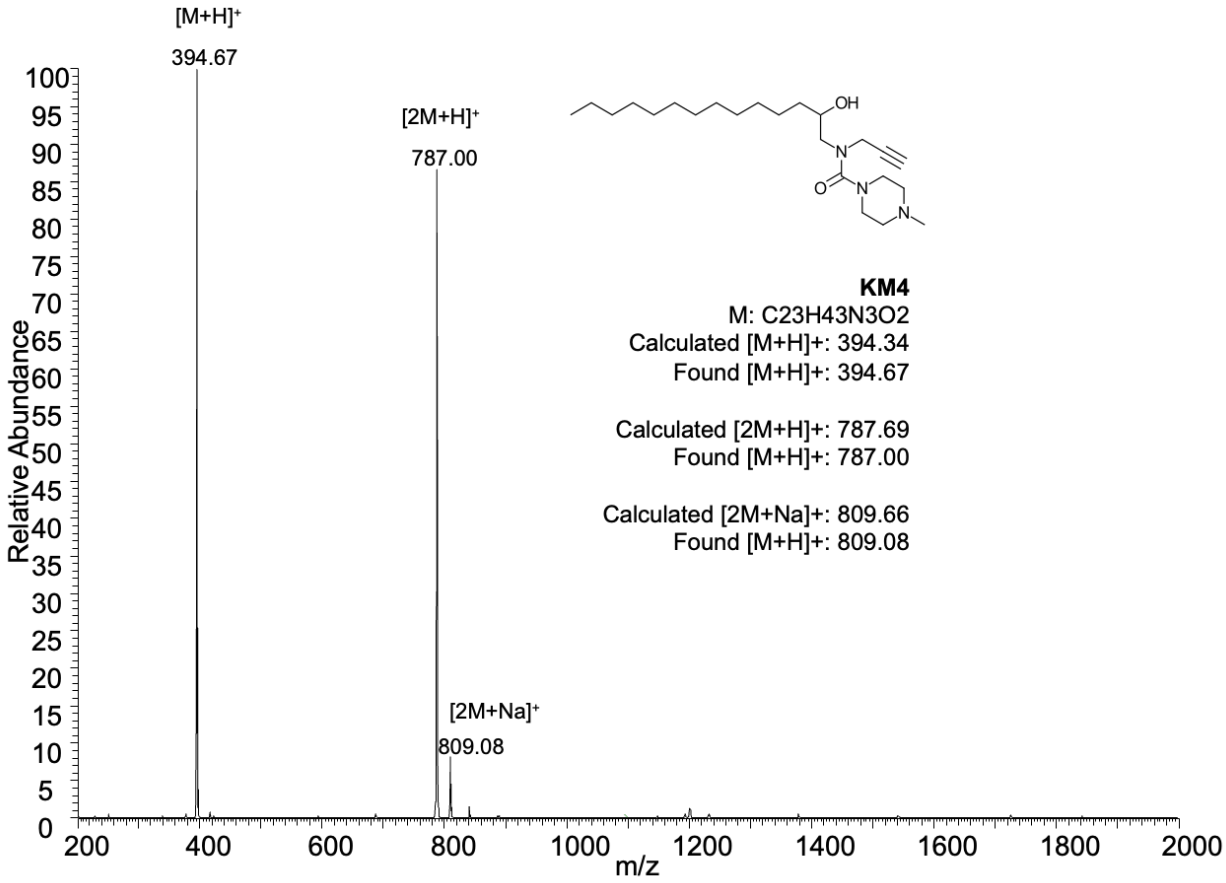

Figure S16. ESI-MS Spectrum of Lipid KM4.

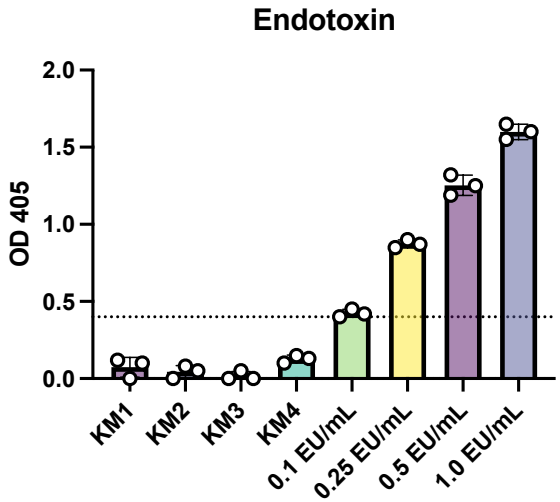

Figure S17. Endotoxin Levels of the KM Lipids.

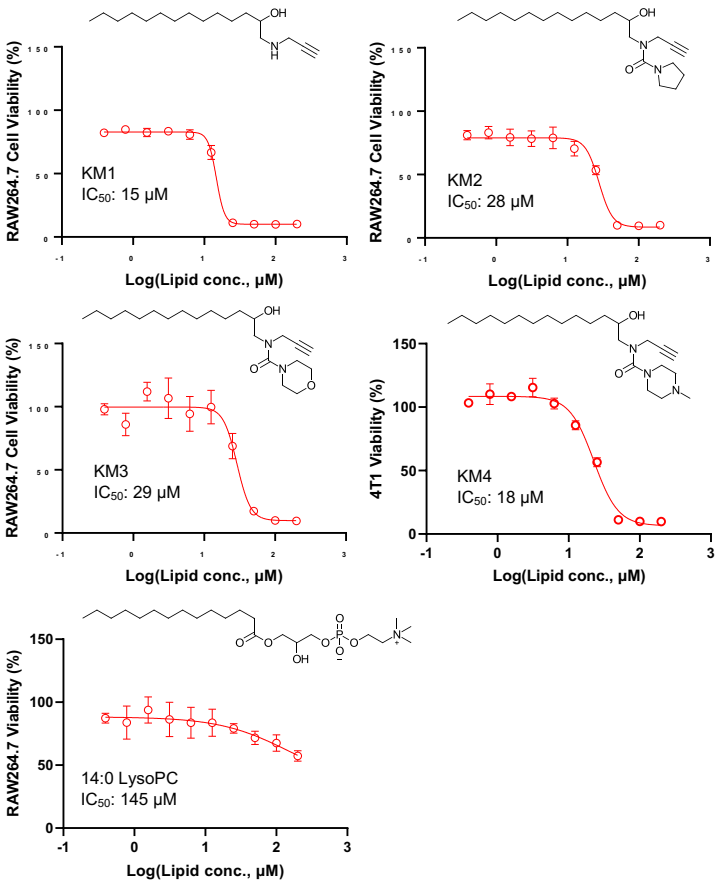

Figure S18. Twenty-four-hour Viability Studies of KM Lipid-treated RAW264.7 Cells.

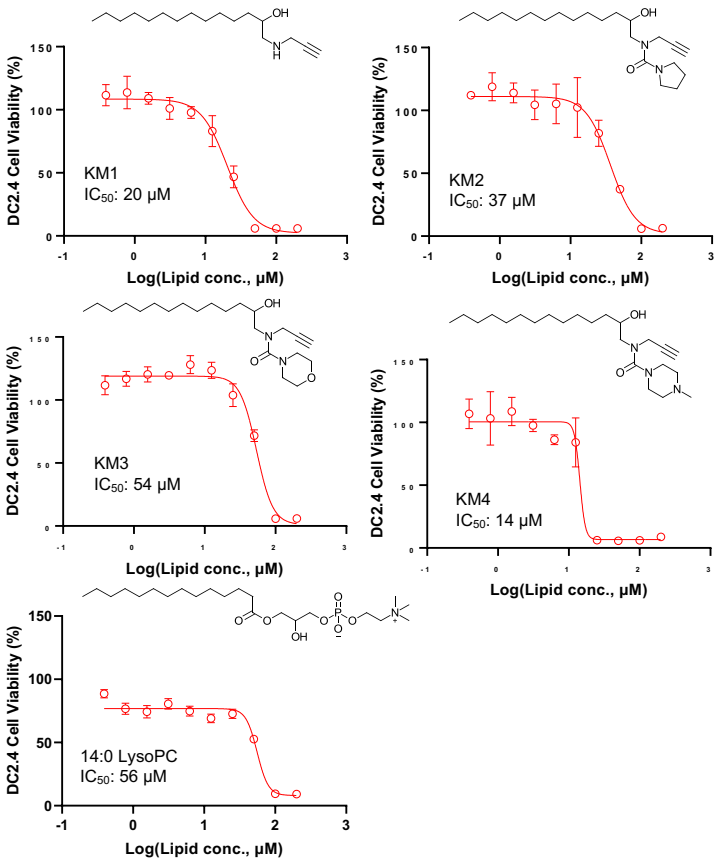

Figure S19. Twenty-four-hour Viability Studies of KM Lipid-treated DC2.4 Cells.

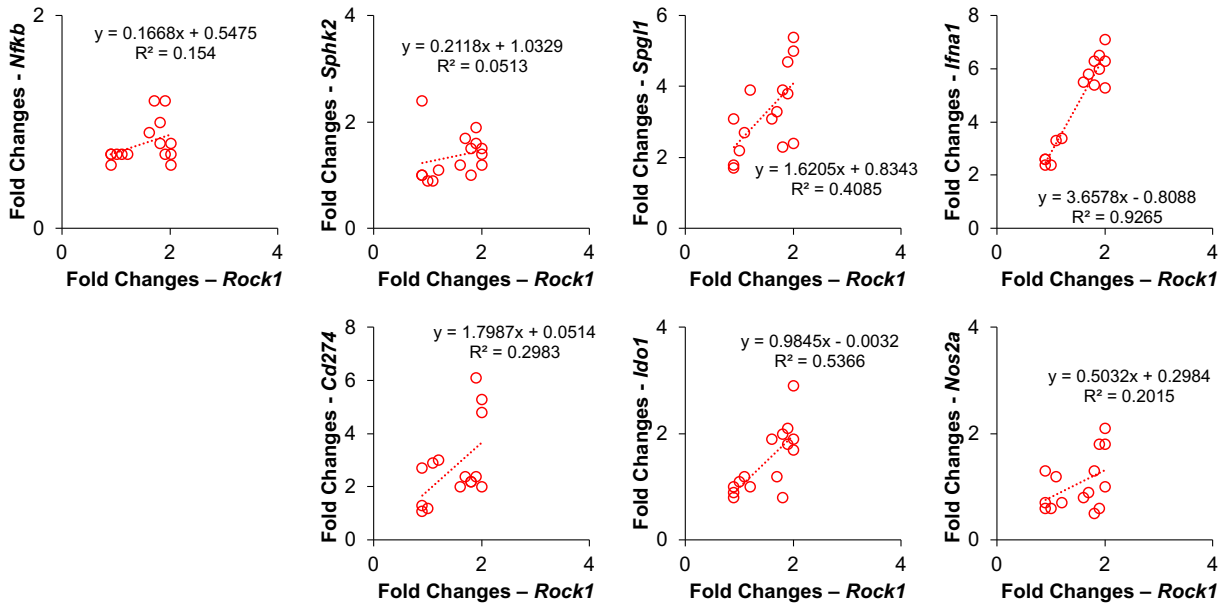

Figure S20. Correlations of Gene Expression Fold Changes as a function of *Rock1* Expression in KM-Lipids Treated RAW264.7 Cells.

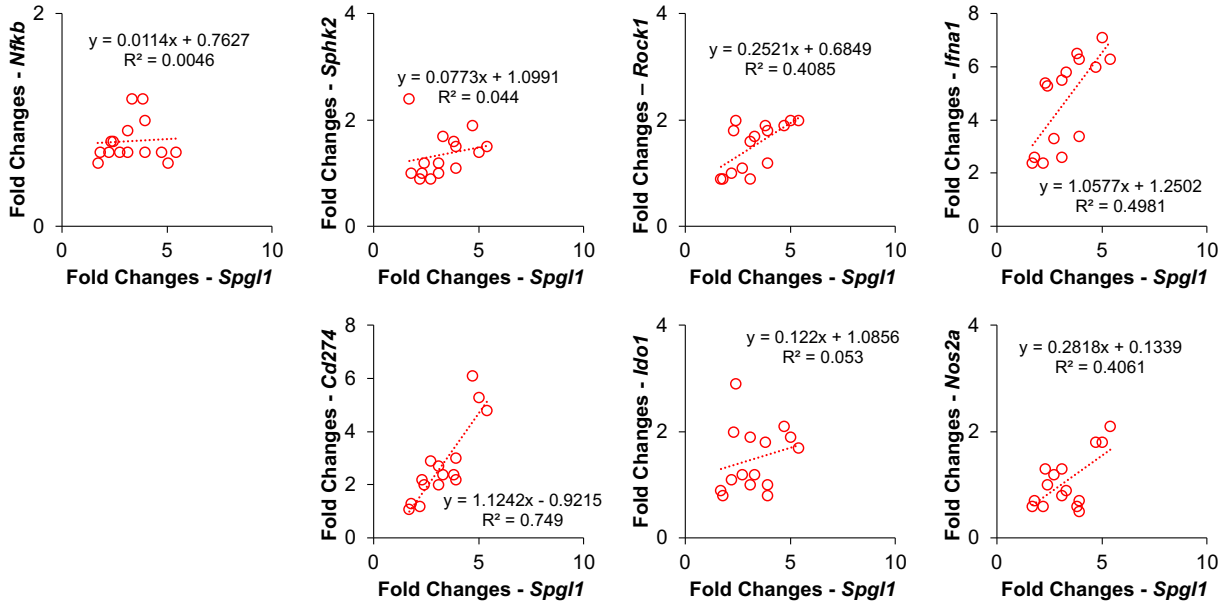

Figure S21. Correlations of Gene Expression Fold Changes as a function of *Spgl1* Expression in KM-Lipids Treated RAW264.7 Cells.

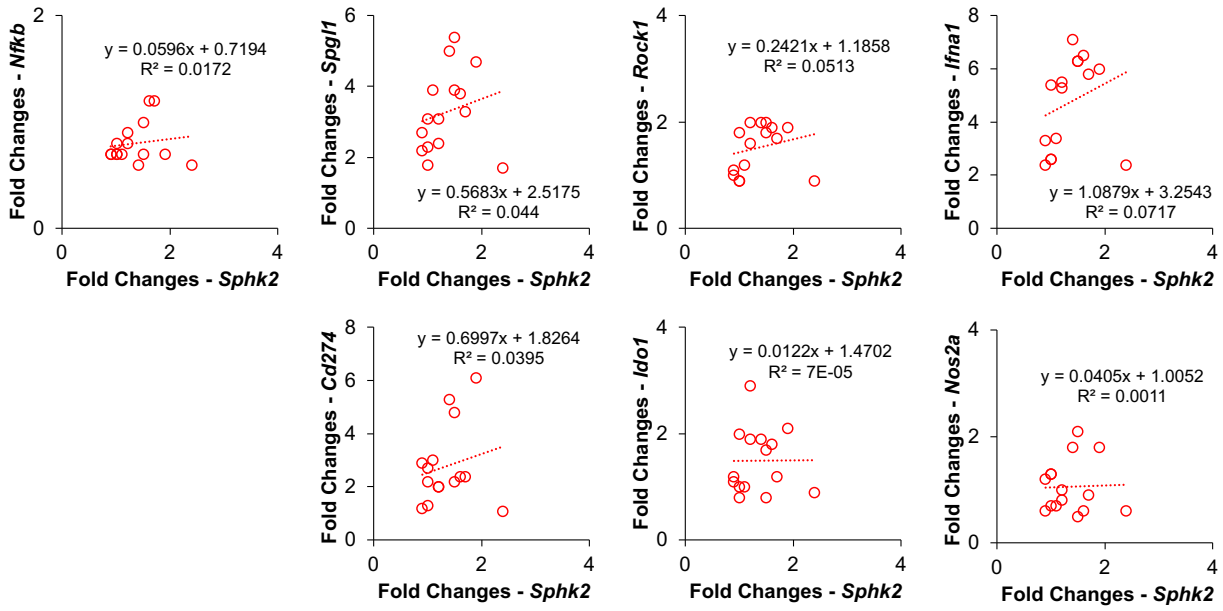

Figure S22 Correlations of Gene Expression Fold Changes as a function of *Sphk2* Expression in KM-Lipids Treated RAW264.7 Cells (continued).

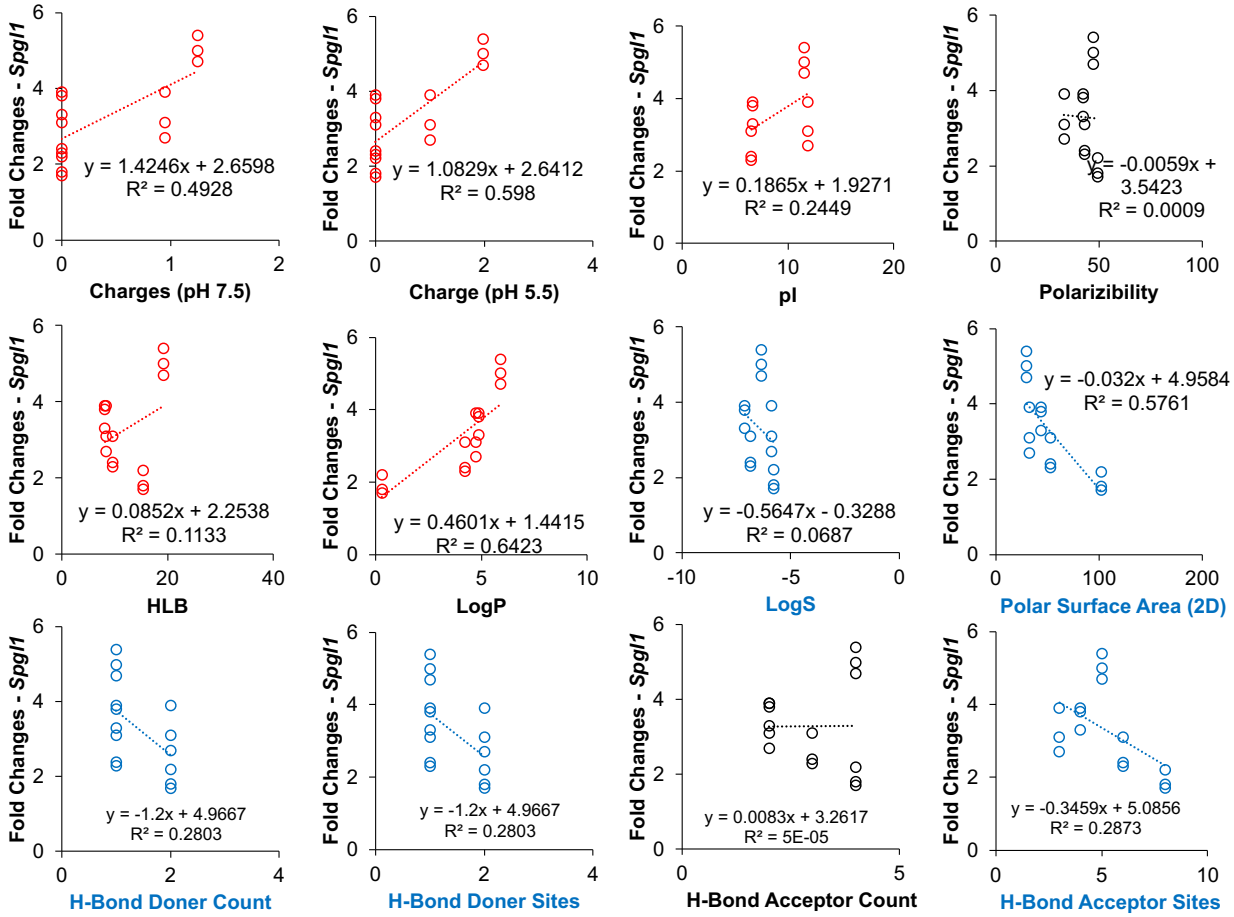

Figure S23. Correlations Between the Physicochemical Properties of the Lipids and *Spgl1* Expression in RAW264.7 Cells.

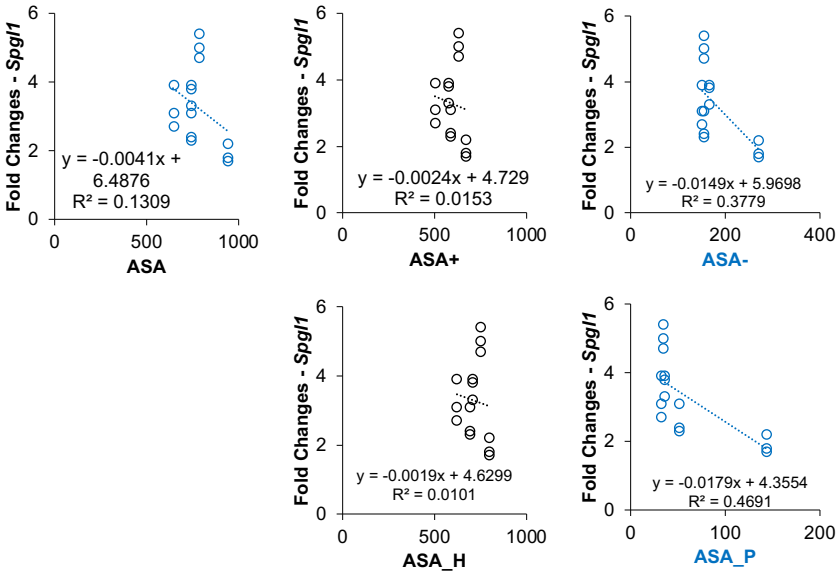

Figure S24. Correlations Between the Physicochemical Properties of the Lipids and *Spgl1* Expression in RAW264.7 Cells (continued).

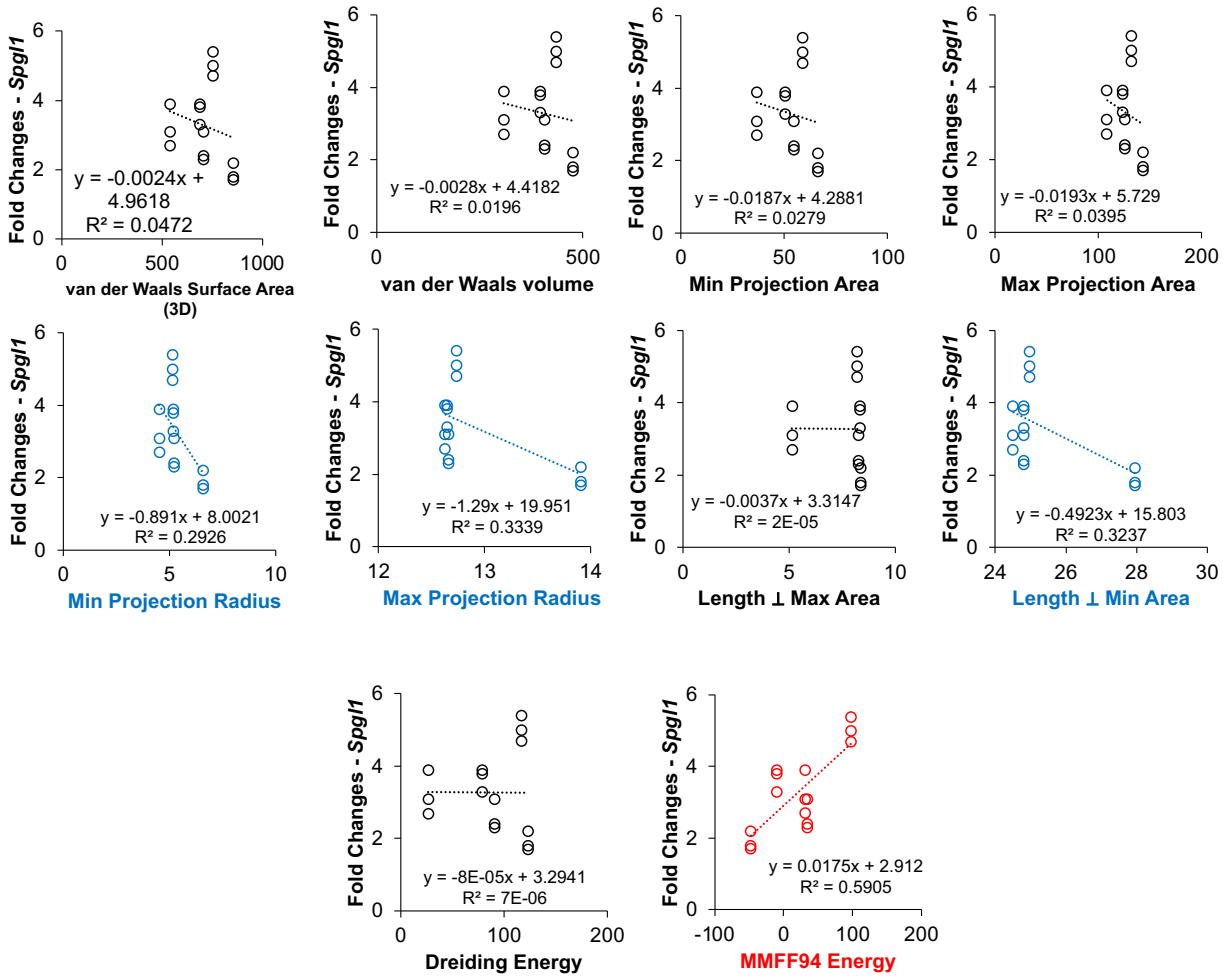

Figure S25. Correlations Between the Physicochemical Properties of the Lipids and *Spgl1* Expression in RAW264.7 Cells (continued).

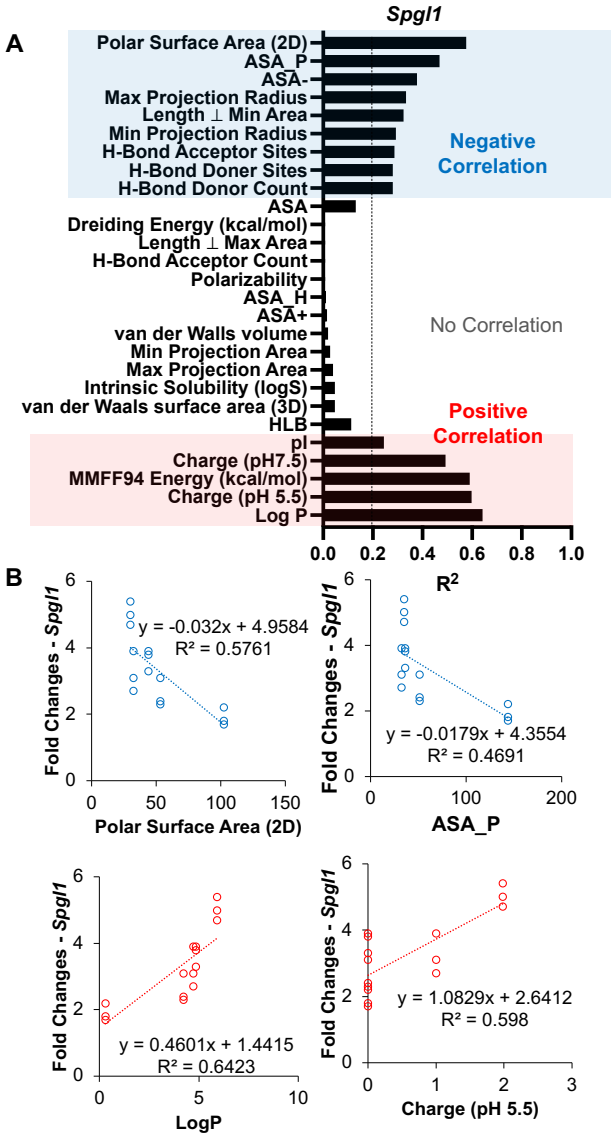

Figure S26. Correlations Between the Physicochemical Properties of the Lipids and *Spgl1* Expression in RAW264.7 Cells (continued).

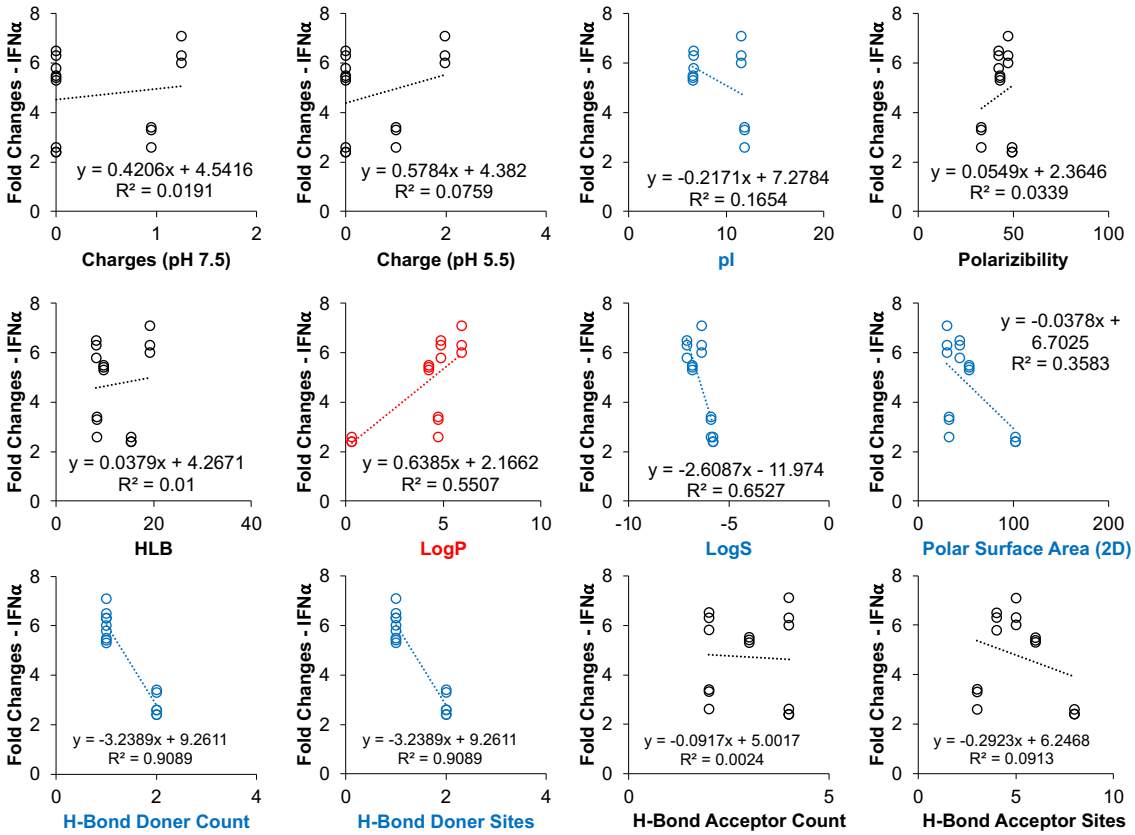

Figure S27. Correlations Between the Physicochemical Properties of the Lipids and *Ifna* Expression in RAW264.7 Cells.

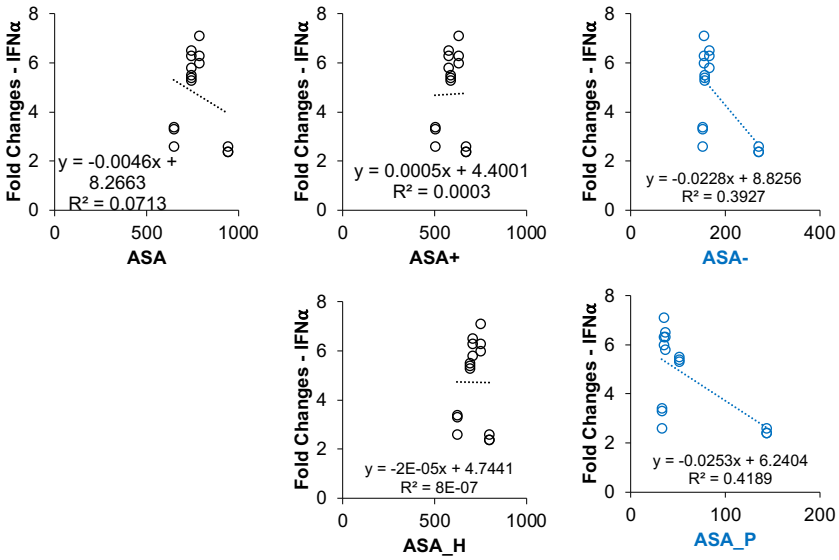

Figure S28. Correlations Between the Physicochemical Properties of the Lipids and *Ifna* Expression in RAW264.7 Cells (continued).

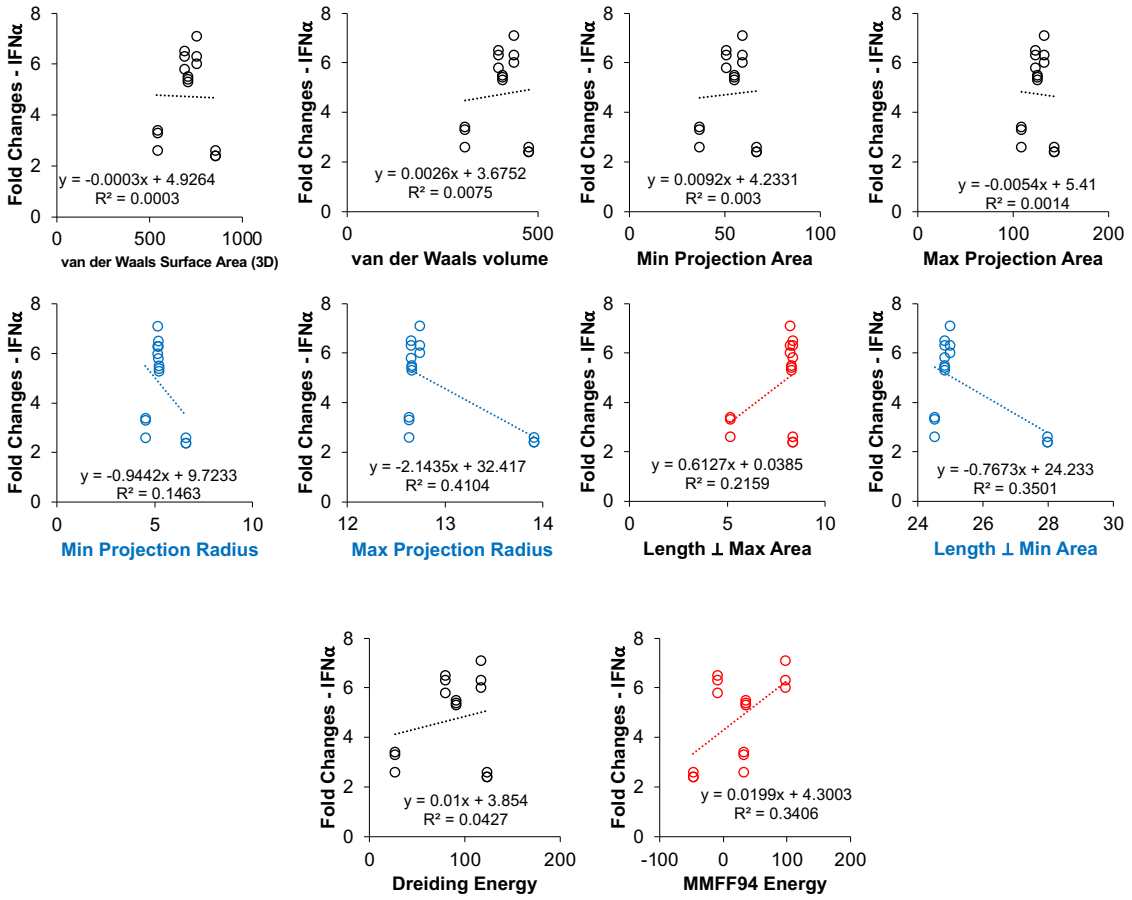

Figure S29. Correlations Between the Physicochemical Properties of the Lipids and *Ifna* Expression in RAW264.7 Cells (continued).

Table S1. PCR Primer Sequences

#	Name	Sequence
0-1	*Gapdh* (forward)	CATCACTGCCACCCAGAAGACTG
0-2	*Gapdh* (reverse)	ATGCCAGTGAGCTTCCCGTTCAG
1-1	*Nfkb* (forward)	CATCACTGCCACCCAGAAGACTG
1-2	*Nfkb* (reverse)	ATGCCAGTGAGCTTCCCGTTCAG
2-1	*Sphk2* (forward)	GGTGCCAATGATCTCTGAAGCTG
2-2	*Sphk2* (reverse)	CTCCAGACACAGTGACAATGCC
3-1	*Rock1* (forward)	CACGCCTAACTGACAAGCACCA
3-2	*Rock1* (reverse)	CAGGTCAACATCTAGCATGGAAC
4-1	*Spgl1* (forward)	GGAAAGCCTCAGGAGCTGTGTA
4-2	*Spgl1* (reverse)	CTGCCTCTAACTTCCGCAATCC
5-1	*Ifna1* (forward)	GGATGTGACCTTCCTCAGACTC
5-2	*Ifna1* (reverse)	ACCTTCTCCTGCGGGAATCCAA
6-1	*Cd274* (PD-L1, forward)	TGCGGACTACAAGCGAATCACG
6-2	*Cd274* (PD-L1, reverse)	CTCAGCTTCTGGATAACCCTCG
7-1	*Ido1* (forward)	GCAGACTGTGTCCTGGCAAACT
7-2	*Ido1* (reverse)	GCAGACTGTGTCCTGGCAAACT
8-1	*Nos2a* (iNOS, forward)	GCAGACTGTGTCCTGGCAAACT
8-2	*Nos2a* (iNOS, reverse)	GCTCTGTTGAGGTCTAAAGGCTCCG

Table S2. Physicochemical Properties of the Lipids.†[1, 2]

	LysoPC	KM1	KM2	KM3	KM4
pI	NA	11.85	6.64	6.55	11.55
Charge (pH7.5)	0	0.95	0	0	1.25
Charge (pH 5.5)	0	1	0	0	1.98
Log P	0.3	4.73	4.86	4.24	5.92
HLB	15.33	8.32	8.12	9.69	19.16
Polarizability	49.27	33.12	42.39	43.08	47.31
Intrinsic Solubility (logS)	-5.8	-5.89	-7.11	-6.85	-6.36
Polar Surface Area (2D)	102.29	32.26	43.78	53.1	29.95
van der Waals surface area (3D, $Å^2$)	851.64	538.6	684.74	702.52	749.62
ASA ($Å^2$)*	942.14	645.15	743.42	742.41	786.35
ASA+**	671.22	502.73	577.23	586.71	631.05
ASA-***	270.93	151.42	166.19	155.69	155.31
ASA_H****	798.11	621.6	707.06	690.91	751.43
ASA_P*****	144.04	32.55	36.36	51.49	34.92
Min Projection Area	66.55	36.73	50.78	54.8	59.18
Max Projection Area	143.38	108.48	123.44	125.67	132.46
Min Projection Radius	6.54	4.49	5.15	5.19	5.09
Max Projection Radius	13.91	12.63	12.65	12.66	12.74
Length ⊥ Max Area	8.35	5.13	8.33	8.25	8.2
Length ⊥ Min Area	27.97	24.51	24.82	24.82	24.99
van der Waals volume	476.06	308.39	396.69	406.9	436.32
Dreiding Energy (kcal/mol)	123.37	26.62	79.34	90.74	116.88
MMFF94 Energy (kcal/mol)	-47.78	31.46	-9.48	34.92	97.77
H-Bond Donor Count	2	2	1	1	1
H-Bond Doner Sites	2	2	1	1	1
H-Bond Acceptor Count	4	2	2	3	4
H-Bond Acceptor Sites	8	3	4	6	5

† Physicochemical properties calculated using Marvin Sketch (Chemaxon)
*ASA: solvent accessible surface area calculated using the radius of the water molecule (1.4 Å)
** **ASA+: ASA of all atoms with positive partial charge (strictly greater than 0)
**ASA-: ASA of all atoms with negative partial charge (strictly less than 0)
**ASA_H: ASA of all hydrophobic atoms
**ASA_P: ASA of all polar atoms

Table S3. PCA Loadings.

	PC1	PC2	PC3	PC4	PC5
Log P	0.19	0.25	0.05	0.15	0.05
MMFF94 Energy (kcal/mol)	0.12	0.28	0.25	-0.42	0.14
Charge (pH7.5)	0.11	0.09	0.42	0.13	-0.28
Charge (pH 5.5)	0.08	0.17	0.42	0.16	-0.57
pI	0.04	-0.06	0.40	0.14	0.71
H-Bond Donor Count	-0.04	-0.38	0.18	0.02	-0.05
H-Bond Doner Sites	-0.04	-0.38	0.18	0.02	-0.05
Intrinsic Solubility (logS)	-0.06	-0.26	0.36	-0.16	0.03
HLB	-0.14	0.19	0.33	0.04	0.07
Length ⊥ Max Area	-0.17	0.26	-0.18	0.10	0.02
H-Bond Acceptor Count	-0.19	0.14	0.23	-0.40	0.04
Dreiding Energy (kcal/mol)	-0.21	0.21	0.03	-0.02	0.03
Polar Surface Area (2D)	-0.22	-0.18	-0.09	-0.16	-0.06
Polarizability	-0.22	0.19	0.01	0.09	-0.02
ASA-	-0.22	-0.19	0.01	0.21	0.01
Max Projection Radius	-0.22	-0.17	0.07	0.09	-0.01
ASA_P	-0.22	-0.18	0.01	-0.12	-0.16
Length ⊥ Min Area	-0.23	-0.15	0.05	0.11	-0.04
van der Waals volume	-0.23	0.15	-0.01	0.04	0.02
Min Projection Area	-0.23	0.15	0.01	-0.08	-0.04
ASA_H	-0.23	0.11	0.05	0.31	0.13
ASA+	-0.23	0.13	0.05	0.07	0.02
H-Bond Acceptor Sites	-0.23	-0.01	-0.03	-0.54	-0.04
van der Waals surface area (3D)	-0.24	0.11	0.00	0.05	-0.04
Max Projection Area	-0.24	0.11	0.03	0.05	0.02
Min Projection Radius	-0.24	-0.07	-0.05	0.06	-0.03
ASA	-0.24	0.00	0.03	0.14	0.03

Table S4. PCA Scores

	PC1	PC2	PC3	PC4	PC5
LysoPC	-6.35	-2.03	0.37	0.05	-5.55E-17
KM1	4.91	-2.74	1.31	-0.04	-2.22E-16
KM2	1.23	0.67	-2.40	0.74	2.78E-17
KM3	0.40	0.99	-1.76	-0.87	3.61E-16
KM4	-0.19	3.11	2.48	0.11	6.51E-17

References:

1. P. Ferrara, J. Apostolakis and A. Caflisch, *Proteins: Structure, Function, and Bioinformatics*, 2002, **46**, 24-33.
2. W. Hasel, T. F. Hendrickson and W. C. Still, *Tetrahedron Computer Methodology*, 1988, **1**, 103-116.